CONF-8304153--2

DE85 004870

DIFFRACTION: WHAT DO WE KNOW; WHAT CAN WE LEARN?*

J. Randa

Physics Department

University of Colorado

Boulder, CO 80309

ABSTRACT

High energy diffractive scattering is reviewed. We first summarize experimental results and information gleaned from geometric and optical models. We then discuss dynamics from the perspectives of hadron structure and Pomeron structure. Particular emphasis is placed on investigating hadron structure using a simple model of the Pomeron.

*Invited talks presented at the XI International Winter Meeting on Fundamental Physics, 11-16 April, 1983, Toledo, Spain.

I. BACKGROUND

A. Introduction

High energy diffractive scattering is a very broad field which could be split into a number of subfields, any one of which could provide sufficient material for a lengthy talk. This superabundance of material is a rather happy circumstance since it means that I can choose to cover those topics which conform to my own prejudices (and which have some nonzero overlap with my knowledge). As you will see, my prejudices in this matter tend toward the simple and basic rather than the intricate and arcane. It is pointless to build phenomenological structures too elaborate and intricate for the theoretical foundations to support. I will concentrate on elastic scattering and the total cross section, with a little attention paid to diffractive dissociation. Other speakers at this meeting have covered multiparticle production [1], and so my emphasis on the elastic amplitude is partly a reflection of what I consider basic and fundamental and partly a search for a vacant evolutionary niche. I also shall not have time to say anything about the very interesting areas of diffractive heavy flavor production or scattering from nuclear targets.

There is a very good reason for our lack of a fundamental understanding of total cross sections, as you all know. Diffraction, being intrinsically a coherent phenomenon, is even more entwined with hadron structure and the problem of confinement than are other soft processes. It is probable that we will not be able to really calculate total cross sections from first principles (i.e. QCD) until after we can calculate the hadron spectrum from QCD. Consequently, all the calculations and insights I talk about will be in the context of models; there are no unassailable QCD calculations. The QCD-based models all use perturbation theory in regimes where it has not been shown to be - and indeed probably is not - applicable.

Despite this warning, I feel we have gained valid insights into diffractive scattering, and have even developed some predictive ability.

For thematic purposes, I shall crudely divide the topics covered into hadron structure and Pomeron structure. This is not possible to do physically, but it is organizationally convenient, and many features are best understood from one or the other perspective. In the remainder of this section we'll review the salient experimental features of diffraction and then summarize the relevance of geometrical models to these features. In the next section we shall adopt a simple model of the Pomeron and show how it allows us to understand total cross sections and to probe hadron structure, after which we'll treat attempts to calculate or model the Pomeron itself. In the final section we shall summarize what has been said and try to collect it all into something resembling a unified picture.

B. Experimental Features

Before embarking on our quest for explanations, it is appropriate to recall just what it is that we are trying to explain. We therefore collect the general features of diffractive scattering which must be explained by a successful model - and a fortiori by the correct theory. Readers who are familiar with the experimental situation are invited to skip to the last paragraph of this subsection.

1) Total cross sections rise slowly with increasing energy, see fig. 1, and in general can be fitted by the form

$$\sigma_{tot}^{aN} = \sigma_0^{aN} + K^{aN} \ln^2(s/s_0) + O(s^{-0.6}). \qquad (1)$$

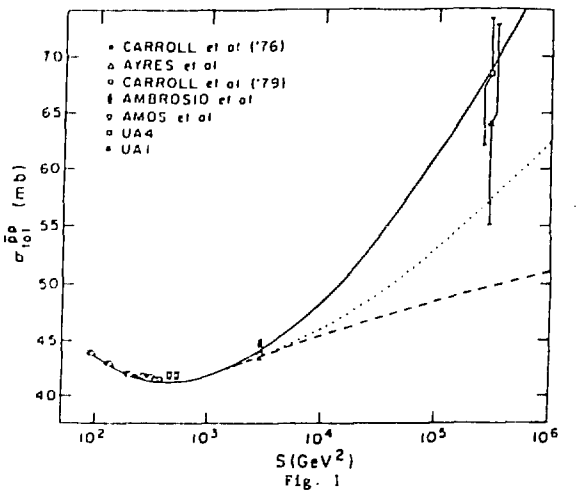

Fig. 1

Total cross section for $\bar{p}p$ as a function of s. Data is from ref. [3,4,5] dotted line is from ref. [6].

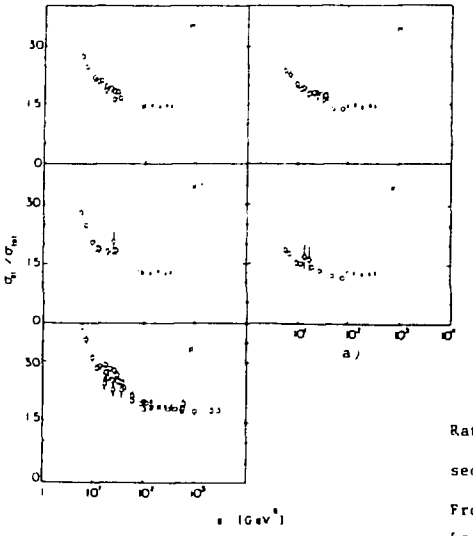

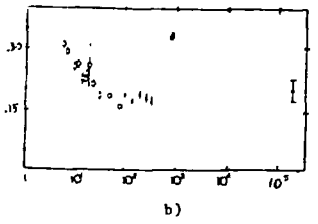

Fig. 2

Ratios of elastic to total cross sections for various beams a) From ref. [7]. b) From ref. [5,7,8]

For $\bar{p}p$ scattering for example, σ_0 = 34.3 mb, K = 0.5 mb, s_0 = 117 GeV^2. Including an $O(s^{-0.6})$ term of 79 mb$(s/GeV^2)^{-0.6}$ gives a good fit through CERN collider energies [2]. The same constants without the $O(s^{-0.6})$ correction fit σ_{tot}^{pp} through the highest ISR energies. The dashed and dotted curves in fig. 1 are respectively a $(\ln s)^{.26}$ dependence and a fit using a critical Pomeron plus nonasymptotic corrections. They are included for later reference.

2) Elastic cross sections also grow slowly with s and are a small fraction of total cross sections. This fraction is s-independent for high energies, $\sigma_{el}^{aN}(s)/\sigma_{tot}^{aN}(s)$ = const = 0.10 - 0.20, depending on the identity of particle a. As can be seen from figure 2, the constant ratio has been achieved for all beams by s = 100 GeV^2.

3) The elastic amplitude is predominantly imaginary. The ratio of real to imaginary parts of the forward elastic amplitude is around 5% at fixed target energies and about 15% at ISR and collider energies [5,8].

4) Elastic differential cross sections are sharply peaked in the forward direction, proportional to exp(Bt) for small t, with the value of B dependent on the beam and on s. As s increases, B rises slowly; for $p\bar{p}$ it goes from 12.6/GeV^2 at $\sqrt{s}$ = 10 GeV [7], to about 13.6/GeV^2 at $\sqrt{s}$ = 53 GeV [9], to around 17/GeV^2 at $\sqrt{s}$ = 540 GeV[5,10]. If we take literally the facts σ_{el}/σ_{tot} = const, $f_{el}(t=0)$ = i Im $f_{el}(t=0)$, σ_{tot} = $\ln^2 s$, and $d\sigma_{el}/dt = \exp(Bt)$, then

$$\sigma_{el} = \int \frac{d\sigma_{el}}{dt}\, dt = \frac{1}{B}\frac{d\sigma_{el}}{dt}(t=0) = \frac{\sigma_{tot}^2}{B} . \qquad (2)$$

In that case σ_{el}/σ_{tot} = const requires σ_{tot}/B = const and therefore B = $\ln^2 s$. Block and Cahn [11] fit B = 10.94 + 0.04 $\ln^2 s$ for $\bar{p}p$ + pp. Their $\ln s$ term is consistent with zero, but a pure $\ln s$ increase for B probably cannot be ruled out.

5) The cross sections display approximate factorization. The prototype test of this would be $\sigma_{\pi p}^2 = \sigma_{\pi\pi}\sigma_{pp}$, but $\pi\pi$ cross sections are not easily measured. In practice, the best evidence for factorization - in both integrated and differential cross sections - probably comes from diffractive dissociation experiments [12].

6) The relative magnitudes of total cross sections for different beams at the same energy display a regularity generally called additivity. As can be seen from Table I, if we take the u, d, s total cross sections on a proton to be σ(up) = σ(dp) = 13 mb, σ(sp) = 5 mb, then the total cross section of a hadron on a proton is given approximately by the sum of the total cross sections of its valence quarks, $\sigma_{tot}(hp) = \sum_{i\in h} \sigma(ip)$ [14]. There are questionable aspects to such an interpretation; but if we wish to discard the notion of additivity, we had better have some other explanation for the relative sizes of total cross sections. And of course I hope to convince you later that we do have a better explanation, otherwise I would not be emphasizing this point now.

Table I: Total cross sections at $\sqrt{s}$ = 13.7 GeV [13]

	pp	πp	Kp	ϕp	Σp	Ξp	$\bar{p}p$
σ_{tot}(mb)	38.4	23.3	18.9	10.5	33.3	29.2	42.0

7) The unitarity sum for the discontinuity in the forward elastic amplitude,

$$\text{Disc}\quad f_{el}^{ab}(t=0) \propto \sum_N \left| f_{ab\to N} \right|^2, \tag{3}$$

is dominated by multiparticle states. When we cut the Pomeron we must reproduce multiparticle spectra correctly. In particular, we must reproduce $\langle n_{ch}(s)\rangle \propto \ell n^2 s$ and $d\sigma(n=0)/dn \propto \ell n\, s$ [15], and approximate KNO scaling [15, 16]

$$\sigma_n \approx \frac{\sigma_{tot}}{\langle n\rangle}\,\psi(z = n/\langle n\rangle). \tag{4}$$

8) Once we have satisfactorily explained all the above features, we can turn our attention to "details" such as: approximate s-channel helicity conservation; the rather small diffractive dissociation cross sections, about $0.15 \times \sigma_{tot}$ for single diffractive dissociation of either particle [17]; selection rules for diffractive excitation; dip position and movement; the break in the diffractive slope, $d\sigma/dt \propto \exp(Bt + Ct^2)$; inclusive spectra, $d\sigma(ab \to aX)/dx \propto (1-x)^{-1}$ as $x \to 1$; etc. Some of these "details" may have obvious explanations; some may actually constitute crucial clues to determining the true mechanism of diffractive scattering.

In summary then, we want our diffractive scattering model to predict total cross sections which grow slowly with s and agree with additivity, elastic cross sections which remain a constant (small) fraction of the total cross sections, and differential cross sections which are exponential in t with a slope whose magnitude increases slowly with s. The elastic scattering amplitude should be dominantly imaginary, should factorize approximately, and its absorptive part should reproduce the known global features of multiparticle events. At the next level of detail, we can worry about helicity conservation, diffractive dissociation and excitation, inclusive

spectra, dip positions, ... In addition, we would expect bonuses in the form of unexpected explanations for old phenomena and/or predictions for new phenomena.

C. Geometry and Optics

Geometrical considerations are included at this point, as an addendum to the experimental features, because they provide a convenient and intuitive way of organizing some aspects of the data. Geometry is not dynamics, but it can show how certain experimental features follow from general geometrical features and point out what properties a successful dynamical model must possess.

The (spinless) elastic amplitude can be written as a Bessel transform of the impact parameter space amplitude,

$$\mathcal{M}_{el}(s,t) = \int_0^\infty bdb\, J_0(bq)\, \mathcal{M}_{el}(s,b)\ ,\quad q = \sqrt{-t}\ , \tag{4}$$

where unitarity allows us to write

$$\mathcal{M}_{el}(s,b) = 4\pi i s\left[1-\eta(s,b)\right]\ ,\quad \left|\eta(s,b)\right| \le 1, \tag{5}$$

with $\left[1-\eta(s,b)\right]$ being called the overlap function.

The optical theorem for our normalization is

$$\sigma_{tot} = \frac{1}{s}\,\mathrm{Im}\,\mathcal{M}_{el}(s,t=0) = 4\pi \int bdb\,\left[1-\mathrm{Re}\,\eta(s,b)\right]. \tag{6}$$

To demonstrate or review the basics of optical models we consider the scattering of waves from a partially absorbing disk of radius R_o. In this case

$$1-\eta(b) = (1-a)\,\theta(R_o-b),\ 0 \le a \le 1, \tag{7}$$

where a = 0 corresponds to perfect absorption. Then

$$\mathcal{M}_{el}(s,t) = 4\pi i s(1-a)\,\frac{R_o^2}{qR_o}\,J_1(qR_o)\ ,$$

$$\sigma_{tot} = 2\pi R_o^2(1-a),\ \sigma_{el} = \pi R_o^2(1-a)^2,\ \sigma_{inel} = \pi R_o^2(1-a^2). \qquad (8)$$

(In such models, where $\eta(s,b)$ is purely real, the elastic scattering arises purely from the shadow of inelastic channels: $\sigma_{el} \to 0$ if $\sigma_{inel} \to 0$.) The ratio of elastic to inelastic cross sections can then be fixed by adjusting a, $\sigma_{el}/\sigma_{inel} = (1-a)/(1+a)$. The characteristic diffractive dip structure arises from the zeros of $J_1(qR_o)$. A dip in $d\sigma/dt$ at $t = -1.5$ GeV^2 would require an R_o of between 0.6 and 0.7 Fm, quite reasonable for the combined hadron radius. Now hadronic matter densities are not theta functions; however the dip structure persists for smoother distributions. Consequently, reproducing the experimental dips - at least qualitatively - is no problem in a model which admits a geometric representation. In addition, use of smoother functions enables one to reproduce forward slopes well. Such distributions can be obtained from quark potential models for hadron spectroscopy, as noted by Gustafson in his talk at this conference two years ago [18]. In addition, such nonrelativistic quark model overlap functions result in kaons being smaller than pions which are smaller than protons, and therefore the correct approximate sizes for total cross sections. We shall return to and belabor this point in the next section.

To see what the actual overlap functions really are, one can invert the Bessel transform, eq. (4), assume that $\eta_{el}(s,t)$ is imaginary, and thereby obtain

$$1-\eta(s,b) = \frac{1}{\sqrt{\pi}} \int q\, dq\, J_o(bq) \left(\frac{d\sigma_{el}}{dt}\right)^{\frac{1}{2}}. \qquad (9)$$

By inserting the measured cross section one obtains the hadron profile in impact parameter space. Plotted in fig. 3, for various beams on a proton target at $\sqrt{s} = 9.7$ and 18 GeV, is $2(1-\eta(s,b))$ [7]. The total cross section

is proportional to the integral over db^2 of the curves in the figure, and so the similarity of the $\sqrt{s} = 9.7$ GeV curves to those at 18 GeV, except for pp and $p\bar{p}$, reflects the fact that the cross sections do not change much between these two energies (a few percent).

We now ask what behavior of $(1-\eta(s,b))$ might cause a rising total cross section. Two simple possibilities are that the range in b could stay the same

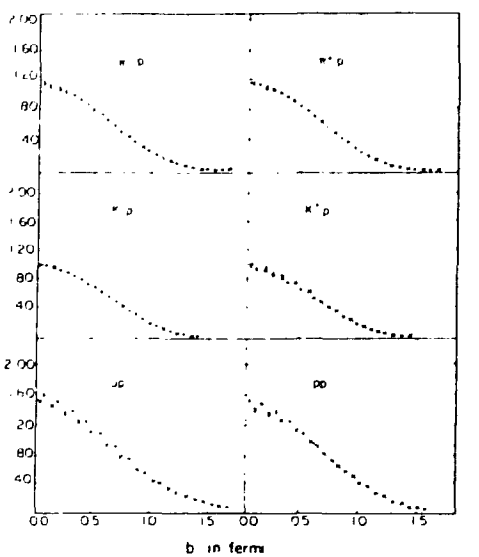

Fig. 3

Plots of $2\pi(1-\eta)$ for various beams at $\sqrt{s} = 9.7$ GeV and 18 GeV; from [7].

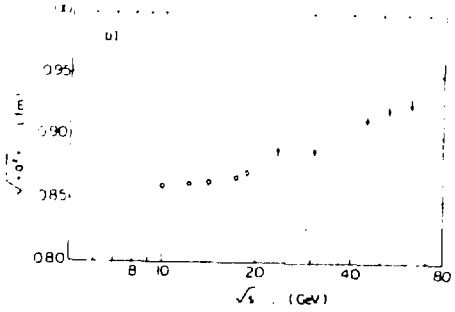

a)

RMS impact parameter for inelastic pp, from [20].

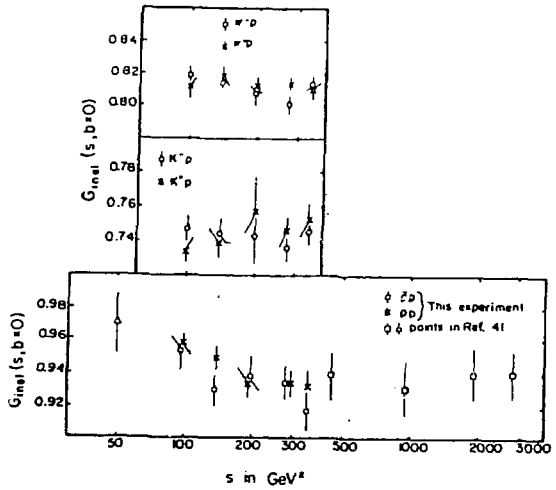

b)

Inelastic overlap function at origin, from [7].

Fig. 4

while the height of the overlap function increased, or the height could stay the same while the range increased. (Obviously any number of combinations of the two are also possible.) Early indications [19] were that the cross section rise was a peripheral phenomenon, and more recent evidence [20] confirms this preference for an increased range. In particular, the rms interaction distance increases with increasing cross section, as can be seen in fig. 4a for inelastic pp processes. On the other hand, the inelastic overlap function at the origin remains roughly constant in the region of rising cross section - fig. 4b, again for pp.

These features indicate that as the energy increases, the overlap function expands, but its central height does not grow. An appealing embodiment of this behavior, which was actually suggested before most of the data became available, is geometrical scaling (GS) [21]. This is the hypothesis that all the energy dependence is contained in a rescaling of the impact parameter scale. In terms of the overlap function, this could be written

$$\eta(s,b) = \eta(b/R(s)),\ \mathcal{M}_{el}(s,b) = s\,m_{el}(b/R(s)). \tag{10}$$

Such a scaling could be imagined occurring in a dynamical model or theory which was sensitive to the transverse size of hadron wave functions, but had an interaction whose range increased with energy.

The consequences of this hypothesis are quite extensive and so far are in agreement with experiment. We first combine eqs. (4) and (10) to obtain

$$\mathcal{M}_{el}(s,t) = sR^2(s)\int_0^\infty x\,dx\,J_0(x \times qR)\,m_{el}(x). \tag{11}$$

It then follows that $\sigma_{tot} = \text{const} \times R^2(s)$, which fixes R(s). It is then easy to show that σ_{el} (and σ_{inel} as well) is a constant fraction of σ_{tot}, as is observed through ISR (and probably collider) energies, cf. fig. 2. Eq. (11)

also indicates that the $t = -q^2$ dependence just gets rescaled by R^2. Consequently the forward exponential slope, $d\sigma/dt = \exp[B(s)t]$ must be proportional to R^2 and therefore to σ_{tot},

$$B(s)/\sigma_{tot}(s) = \text{constant}. \tag{12}$$

Similarly, the dip position also scales with R^2,

$$t_{dip}\, R^2(s) = \text{const}. \tag{13}$$

The slope variation is experimentally confirmed through ISR energies, as is shown in Fig. 5. The dip movement is in qualitative agreement with the prediction at collider energies [5]. In addition, geometrical scaling leads to constant $\langle b^2\rangle/\sigma_{tot}$ and $\eta(s,b=0)$, which were discussed above.

The alternative geometrical mechanism for accounting for the rise in σ_{tot} is a blackening of the center of the hadronic disk, as proposed in the Chou-Yang (CY) model [22]. Such a mechanism has problems with the observed dip motion and constancy of $\eta(s,b=0)$. Other important tests are predictions for σ_{el}/σ_{tot} and B/σ_{tot}. At $\sigma_{tot} = 60$ mb, σ_{el}/σ_{tot} is predicted

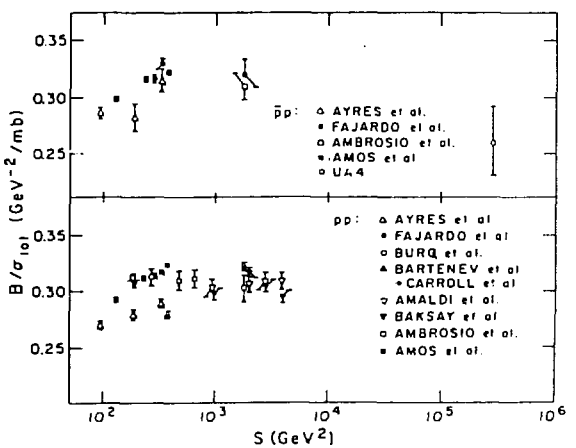

Fig. 5

to be .22 - .23 by CY [22b], and about .18 from GS. The collider measurement is 0.20 ± 0.02 [5]. For B/σ_{tot} (in GeV^{-2}/mb) CY predicts about .23 and GS expectations are about .31, whereas the data say 0.26 ± 0.025. More precise measurements of these two quantities and a determination of $\eta_{inel}(b=0)$ at collider energies will determine which geometrical mechanism is closer to the truth.

The successes of geometrical and optical models are too widespread and too natural to be coincidence. They indicate that a successful model should admit a geometrical interpretation or representation and that, conversely, any model which does reduce to an optical form will have many (at least qualitatively) correct features.

So why should we bother studying diffraction at all, what else can we learn? The first point is that optical models do not "explain" elastic scattering in any fundamental way - they cannot since they are devoid of any dynamics. It helps to recall that no one has told us that the scattering amplitude must be proportional to the overlap of matter densities. The challenge is to obtain a model with geometrical features which is based on (derived from, ideally) a fundamental theory with point-like constituents. In addition, we must also understand the origin of the s dependence of the scattering mechanism. And finally, there is the question of hadron structure. Just as x-ray diffraction may not directly imply Maxwell's equations but does yield information about the target's structure, so too with hadronic diffraction we can learn something of hadron structure. And because we have the possibility of exciting the target or beam, we can learn more than just the hadrons' sizes.

II. TWO - GLUON EXCHANGE (2GE)

In this section we shall adopt a simple model for the Pomeron and concentrate on what we can learn about hadronic structure, and what features of diffractive scattering can be understood from this perspective.

A. Total Cross Sections

Study of the Pomeron in QCD got off the ground in 1975 with the work of Low and Nussinov [23]. They suggested that since the Pomeron corresponds to vacuum quantum number exchange it should be built from multiple gluon exchange in QCD. We briefly recall Low's treatment as a bit of a prelude. Two color singlet hadron bags, to which are confined the colored quark and gluon fields, approach each other as in fig. 6a. As they overlap, a right- and a left-moving quark exchange a gluon, fig. 6b, leaving two color octets receding from one another, connected by a tube of flux, fig. 6c. As the octets recede farther, more and more energy is contained in the connecting fields, and it becomes energetically favorable to produce a $q\bar{q}$ or gg or $qqq\bar{q}\bar{q}$, fig. 6d. (For simplicity fig. 6d was drawn as if gg or $qqq\bar{q}\bar{q}$ were pulled from the vacuum. If it were $\bar{q}q$ there would be a triplet and antitriplet receding,

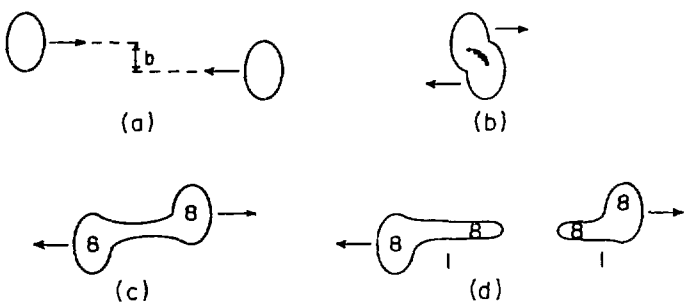

Fig. 6

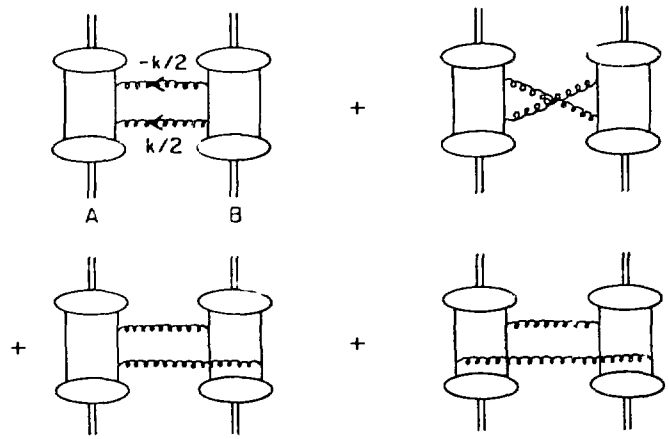

Fig. 7

which could then reach the configuration pictured by producing another $q\bar{q}$.) This process then repeats itself within each of the resultant subsystems. Low estimated the separation distance for producing pairs from the vacuum, based upon the bag model, and used the recursive behavior of the fragmentation to derive a $\ln s$ behavior for the multiplicity. It is clear that once the original color exchange occurs, one is free to insert one's favorite hadronization model, a point to which we shall briefly return below. One qualitative property which immediately follows from this picture is that the elastic cross section will be but a small fraction of σ_{tot} since fig. 6c will usually result in a multiparticle state. An obvious theoretical problem is the first/then dichotomy, first gluon exchange, then hadronization. As Low noted, there are not two different time scales, one much shorter than the

other, and consequently there is not a clear distinction between the perturbative scattering and the nonperturbative hadronization. This is just a manifestation of the inability to justify perturbation theory for such processes, as noted in the Introduction.

It is nevertheless interesting to pursue such a model further. The lowest order contribution to the elastic scattering amplitude is two gluon exchange (2GE), shown in fig. 7 for meson meson (MM) scattering. Gunion and Soper [19] were the first to consider this quantitatively, finding a number of attractive features and an appealing physical picture. The forward elastic amplitude is found to be

$$\mathcal{M}_{el}(t=0) = \frac{is}{8\pi^2}\left(\frac{4g^2}{3}\right)^2 \int d^2k \left[(\vec{k}/2)^2 + \mu^2\right]^{-2} 2\left[1 - f_A(\vec{k}^2)\right] \times 2\left[1 - f_B(\vec{k}^2)\right], \tag{14}$$

where f_A and f_B are form factors calculated by taking the expectation value of $\exp[i\vec{k}\cdot(\vec{x}_1-\vec{x}_2)]$ in the ground state of mesons A and B. The vector k has transverse components only, the energy and longitudinal integrations having already been performed. The gluons are given a fictitious mass μ for manipulative convenience. The integral is finite for $\mu^2 = 0$, and μ^2 is set equal to zero at the end of the calculation. The fact that the amplitude is finite for $\mu = 0$ is itself encouraging, since 2GE leads to a divergent quark-quark or quark-meson amplitude.

Some of the virtues of eq. (14) are obvious. It is pure imaginary; real parts must arise from higher order corrections. It leads to a total cross section which is constant in s— not the $\ln^2$s exhibited by the data, but close enough for the lowest order. A fact which is not obvious from eq. (14) is that the amplitude is pure helicity nonflip, due to the manner in which vectors couple to high energy fermions. A nice geometrical picture is

suggested if we consider the behavior of $\mathcal{M}_{el}$ as the size of one meson goes to zero. If the wave function is nonvanishing only within $x < R$, and $R \to 0$, then

$$(1 - f_A) \sim \int d^2x \left|\psi(x)\right|^2 \left[1 - \exp(i\,\frac{\vec{k}}{2}\cdot\vec{x})\right]$$
$$= \frac{1}{8}\int d^2x \left|\psi(x)\right|^2 (\vec{k}\cdot\vec{x})^2 \sim \langle r^2\rangle \tag{15}$$

(for an $\ell = 0$ meson), and the cross section vanishes as the cross sectional area. The lowest color multipole of an $\ell = 0$ color singlet is its quadrupole moment, which vanishes ($\sim R^2$) as the size of the meson goes to zero. A pointlike gauge singlet does not radiate gauge bosons. An additional point is the relationship between meson meson (MM), meson baryon (MB), and baryon baryon (BB) cross sections. If particle A is a baryon rather than a meson, then $2[1-f_A] \to 3[1-f_A]$, and the same for particle B if it is a baryon. The form factor f_A is $\frac{1}{3}\sum_{i\neq j} \langle\exp(i\vec{k}\cdot(\vec{x}_i-\vec{x}_j))\rangle_{G.S.}$, where i, j are valence quarks of the baryon. The factor of 3/2 arises from the color sums, and could account for the ratio of $\sigma_{tot}(pp)$: $\sigma_{tot}(\pi p)$ - provided the wave functions of quarks in baryons and in mesons are similar. (Lipkin has shown that the same factor also arises for three gluon exchange [25].)

The obvious question then is whether this model leads to reasonable results for the relative magnitudes of total cross sections. Gunion and Soper noted that for weakly bound quarks of equal mass the f_A's can be approximated by electromagnetic form factors, and they used a model for form factors to estimate cross section predictions for various mesons. We shall adopt a different tactic, which is to use a set of hadron wave functions to explicitly calculate the f_A's and hence the total cross sections [26]. For the meson wave functions we choose to use Gaussians, corresponding to a harmonic oscillator potential. The coefficient in the exponent is fixed by the

requirement, gleaned from leptonic decays of vector mesons, that the wave function at the origin is proportional to the mass of the vector meson. This fixes the meson wave function:

$$\psi_M(x) = (\beta_M^2/\pi)^{3/4} \exp(-\tfrac{1}{2}\beta_M^2 x^2),\ \beta_M^2 = a^2 \bar{m}_M^{4/3}, \qquad (16)$$

where $\bar{m}_M$ is twice the reduced mass for the system and "a" is the same for all mesons - and baryons. Requiring that the qq potential is the same as that for $q\bar{q}$, except for gauge group factors of course, then determines baryon wave functions as well. See e.g. [27,28] for details. For baryons with three equal mass (m_q) quarks the wave function is

$$\psi_B(\rho,\lambda) = (\beta_B^2/\pi)^{3/2} \exp\left[-\tfrac{1}{2}\beta_B^2\,(\rho^2+\lambda^2)\right],$$

$$\vec{\rho} \equiv (\vec{x}_1 - \vec{x}_2)/\sqrt{2},\ \vec{\lambda} \equiv (\vec{x}_1 + \vec{x}_2 - 2\vec{x}_3)/\sqrt{6},$$

$$\beta_B^2 = 3a^2 m_q^{4/3}. \qquad (17)$$

If two quarks have mass m_q and one has m_q', it is

$$\psi_{B'}(\rho,\lambda) = \left(\frac{\alpha_\rho \alpha_\lambda}{\pi^2}\right)^{3/2} \exp\left[-\tfrac{1}{2}(\alpha_\rho^2\rho^2 + \alpha_\lambda^2\lambda^2)\right],$$

$$\alpha_\rho^2 \equiv 3a^2 m_q^{4/3},\ \alpha_\lambda^2 \equiv 3a^2 m_\lambda^{4/3},\ m_\lambda \equiv \frac{3m_q m_q'}{2m_q + m_q'} \quad . \qquad (18)$$

The factor of 3 between β_M^2 and β_B^2 is due to there being three interacting qq pairs in a baryon and only one $q\bar{q}$ pair in a meson. These wave functions are obviously not meant to reproduce hadron spectroscopy, but do possess a number of realistic features and are convenient for our purposes. Oscillator wave functions are the starting point in the very successful potential model of Isgur and Karl [28,29]. We have just modified their β's so that $\psi_M(o) \sim m_M$. Our modification is meant to be a crude incorporation of other effects, such

Table II: Predicted and observed total cross sections at $\sqrt{s}$ = 13.7 GeV. Experimental results from [13].

σ_{tot}(mb)	pp	-p	Ξp	Ωp	ππ	πp	Kp	φp	ψp	Dp
pred.	(38.4)	35	31	27	15	24	20	16	7.2	11
expt.	38.4	33.3	29.2	--	--	23.3	18.9	10.5	2	--

as the 1/r attraction which is more important for larger masses, while still retaining the simplicity of Gaussians.

We insert these wave functions into eq. (14) and use the optical theorem (6) to obtain total cross sections for MM, MB, BB. Since the hyperon total cross section measurements are at $\sqrt{s}$ = 13.7 GeV [13], we use $\sigma_{tot}(pp)$ = 38.4 mb [13] to fix g^4/a^2, which multiplies each cross section. This yields the results of Table II. Except for φp and ψp, to which we shall return, the agreement is very good, within 8% in every case. Thus the 3:2 baryon: meson ratio obtained just from the SU(3) algebra survives approximately (πp/pp = 0.62), and in addition we have obtained the correct qualitative and even quantitative suppression of cross sections for hadrons containing strange quarks - without resorting to different u and s cross sections. We've used 2GE plus Gaussian wave functions fixed by spectroscopic constraints. The Σp cross section is smaller than that for pp not because the strange quark's cross section is smaller than the u's, but because the sigma is smaller than the proton. Bound states of heavy quarks are smaller than light quark bound states, and 2GE translates that into smaller cross sections. We thus seem to have a derivation of the relative magnitudes of hadron cross sections and are free to discard the notion of incoherent sums of quark proton total cross sections.

What about ϕp and ψp? The predicted cross sections are small, but not small enough: the ϕp prediction is about 50% too large, and that for ψp is a factor of 2-4 too high. This isn't too worrisome since we know that the charmonium spectrum is characteristic of an r^{ν} potential with ν small (0-.2) [30] and is therefore poorly represented by a Gaussian. The same is probably true to a lesser extent for the ϕ. Results for the lighter states are sufficiently good to warrant further investigation using a better set of wave functions. They also suggest that total cross sections are sensitive to hadron structure and are another piece of information which could be considered in models for hadron wave functions. This could be premature, however, until one also understands t distributions in this context. (See comment below.)

If the D wave function is also much different from a Gaussian, it could bring down the Dp prediction to well below the additive quark model prediction (~13 mb). For a heavy quark Q, additivity would prevent the $M(\bar{Q}u)$-proton cross section from falling below about $\frac{1}{2}\sigma_{tot}(\pi p)$ as $m_Q \to \infty$. With 2GE the total cross section for $M(\bar{Q}u)$-p would also approach a constant as $m_Q \to \infty$, since then the meson size would be determined entirely by the light quark; but the constant is lower than $\frac{1}{2}\sigma_{tot}(\pi p)$. Measuring $\sigma_{tot}(Dp)$ could be rather challenging. There is a suggestion to extract it from the nuclear A dependence of D production, but it is not at all clear that the D is formed within the nucleus. Rather there are indications [31] that the dressing or hadronization of produced quarks at high energies occurs on a length scale greater than or comparable to nuclear sizes.

An additional feature of note is that approximate factorization is obtained. Using the predictions in Table II, $\sqrt{\sigma_{\pi\pi}\sigma_{pp}} = 23.7$ mb, to be compared with 24 mb predicted for $\sigma_{\pi p}$. This feature will also carry over to diffractive dissociation, which will be discussed in the third part of this section.

There are a number of other possible calculations and comparisons which spring to mind. Total cross sections for radial recurrences of vector mesons could be calculated. The ratios $\sigma(V'p)/\sigma(Vp)$ for ρ', ω', ϕ', ψ' can be extracted from photoproduction [32] if we know the relevant branching ratios and $\gamma V'$ couplings from e^+e^-. [Working with ratios of cross sections reduces the uncertainty introduced by using $f_V(q^2 = m_V^2)$ instead of $f_V(q^2=0)$.]

Another open problem is that elastic differential cross sections have not been calculated yet in this model. However, t distributions are much more sensitive to higher order or nonperturbative effects than are the forward amplitudes [24,33]. Consequently we cannot yet address the question of the forward slope or quantitative prediction of the σ_{el}/σ_{tot} ratio. This is obviously an important point, as is the question of generating the $\ln^2 s$ increase in σ_{tot}. It is quite possible that they both involve the same corrections to 2GE.

B. Significance

The biggest question posed by the previous subsection would seem to be why 2GE should work at all. The answer is that we don't really know (yet), but there are two possibilities which come to mind - one mundane, the other more speculative. The safe, boring explanation is that hadron total cross sections are determined mostly by hadron sizes, and 2GE just happens to reflect hadron sizes. Consequently the 2GE prediction is proportional to the total cross section.

The second, more interesting, scenario is called to the attention of less cautious readers. If a two-phase picture of the hadronic vacuum is adopted, free space has a nonperturbative superconductor-like vacuum which excludes

color fields. Consequently, only (real or virtual) color singlets can propagate in free space. Within a hadron, on the other hand, is a region of space with a normal perturbative vacuum, in which color fields can propagate. Nonperturbative effects keep quarks from escaping from hadrons, but within hadrons quarks and gluons interact perturbatively. Such a picture underlies successful spectroscopic models with a confining interaction (bag pressure [34], potential [27,28]). It is not that intrahadronic distances are small enough to justify perturbation theory - from fig. 4a we see that typical interaction distances are around 0.8 Fm $\sim$0.25GeV. However, it may be that nonperturbative effects enter almost exclusively as a confining potential and that to a good approximation they can be contained in the wave functions.

The important mechanism for hadron scattering then depends on impact parameter. For small impact parameter, the two hadrons overlap significantly and partons from the two hadrons are in the same continuous volume of perturbative vacuum, cf. fig. 6. They interact perturbatively and separate as in Low's picture. If the perturbative interaction resulted in 'eft- and right-moving color singlets, then they separate without nonperturbative interaction - except within each separately of course. For large impact parameter, the two colliding hadrons do not overlap, and whatever is exchanged between them must propagate through the nonperturbative vacuum. We therefore expect such interactions to be mediated by exchange of color singlet hadrons - mesons, baryons, glueballs. Since diffractive scattering is dominated by small impact parameter a perturbative approximation could work for it, whereas for the more peripheral quantum number exchange reactions or for the large impact parameter part of the Pomeron (glueballs?), nonperturbative methods could be required. (Even for the perturbative case, it is likely that we need to include other exchanges - e.g. ladders.)

In any case, whether the success of 2GE for total cross sections is significant or fortuitous it is clear that diffractive scattering is intrinsically bound up with hadron structure and therefore constitutes a probe of it. If 2GE is in fact a good approximation, then we understand the probe and can begin using it to extract information.

C. Diffractive Dissociation

The 2GE treatment of the elastic amplitude can be extended to diffractive excitation, ab + a*b, and diffractive dissociation, ab + Xb. For diffractive excitation all that is required is the change of a final state wave function. Such a calculation would allow a derivation of selection rules for diffractive excitation. Because the $\psi^*_{a^*}\psi_a$ overlap is now important, it would require believable wave functions. Any real comparison to experiment would also require t dependence, and that remains to be done. There is some work on forward cross sections [35], but the surface has barely been scratched. For inclusive diffractive dissociation, there has been work on the normalization of integrated cross sections [33,36], as well as the work described below. (Note that [36] is not really 2GE; it is a modified Abelian model with a particular prescription for confinement effects.)

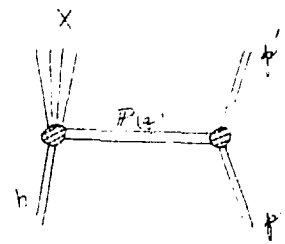

Fig. 8

We shall concern ourselves with high-mass diffractive dissociation [37]. In order that an event be identified as diffractive dissociation, we require a large rapidity gap between the subsystem of projectile fragments and the remainder of the particles produced - e.g. from target fragmentation. For simplicity we shall treat the case of an elastic recoil proton, but because of the approximate factorization which occurs it would be trivial to extend the treatment to cases in which the proton also dissociates.

The process we consider then is hp → Xp as pictured in fig. 8, where the particles in X are all forward ($\vec{p}_i \cdot \vec{p}_h > 0, i \in X$) in the overall center of mass. As a matter of notation, we shall use an asterisk to denote variables measured in the $\vec{p}_X = 0$ frame or internal to the X subsystem (e.g. $s^* = M_X^2$, etc.). If we assume 2GE for the Pomeron, the amplitude is given by

$$\mathcal{A}(hp \to Xp) = \frac{is}{2}\left(\frac{4g^2}{3}\right)^2 \int \frac{d^2q_1 d^2q_2}{(2\pi)^2}\, \delta^2(q-q_1-q_2)\, q_1^{-2} q_2^{-2}\, \hat{L}\, \hat{R},$$

$$q^2 = t, \tag{20}$$

where $\hat{L}$ is the amplitude for $g(q_1)\, g(q_2)\, h \to X$. $\hat{R}$ is the ppgg vertex, $\hat{R} = [f_1(q) - f_2(q_1,q_2)]$, where f_1 is a form factor for 2GE from the same quark line in the hadron, and f_2 is a form factor for 2GE from different lines. For $q = 0$, $\hat{R}$ reduces to $[1 - f_p(q_1)]$, as in eq. (14). For $x \neq 1$, eq. (20) can be written approximately in a factorized form, and $\hat{L}$ can be simply related to $\mathcal{A}(h\bar{p} \to X)$. This leads to the form

$$\frac{d\sigma(hp \to Xp)}{dt\, dM^2} = (32\pi^2)^{-1}\, F^2(q,x)\, \sigma(h\bar{P} \to X),$$

$$F(q,x) \underset{x\neq 1}{\longrightarrow} F(q) = \int \frac{d^2k}{(2\pi)^2}\, (\vec{k}+\vec{q}/2)^{-2} (\vec{k}-\vec{q}/2)^{-2}\, \hat{R}, \tag{21}$$

where F^2 may be thought of as a fragmentation function for $p \to \bar{P}p$. For $x = 1$, if one insists on the factorized form of eq. (21), then F^2 diverges as

$(1-x)^{-1}$. This is the appropriate behavior for a diffractive fragmentation function and it reproduces the correct exclusive limit, cf. [38]. Eq. (21) was derived in a 2GE model of the Pomeron, but it is considerably more general than that model. The only features we have really exploited are the approximate factorization and that the Pomeron is a spatially extended color singlet coupling nonlocally to the constituents of p and h. Eq. (21) can also be made differential in any variables of the $h\bar{P} \to X$ subprocess.

What do we expect of the $h\bar{P}$ cross section? Like all other hadronic total cross sections it should be asymptotically constant (modulo logs). That and $F^2(x,q) \sim (1-x)^{-1}$ lead to $d\sigma/dM^2 \sim M^{-2}$ for all h, in agreement with experiment [39]. It will be dominated by soft hadronization, two hadronic jets with an exponential distribution of the jet axis direction about the $h\bar{P}$ axis. Fast hadrons (in the $h\bar{P}$ CM) in the jet oriented along the beam direction arise from the fragmentation of h; fast hadrons following the Pomeron's direction arise from Pomeron fragmentation, fig. 9a. A central plateau will appear for large enough $s^* = M_X^2$. Such events will reflect pointlike dynamics only indirectly, perhaps in the x_F^* dependence of h or $\bar{h}$ fragmentaiton, but not in the jet axis distribution.

There is also a (smaller) component of $h\bar{P}$ scattering which involves large momentum transfer and which may therefore reveal pointlike dynamics in h. The subprocess which as been studied [40] is meson (M) or photon + $\bar{P} \to q+\bar{q}$, fig. 9b, where 2GE is used for the $\bar{P}$, and the contributing diagrams are shown in fig. 10. Use of 2GE for this process is a bit more solid than for elastic scattering since large $t^* = (p_1-k_1)^2 \approx \frac{s^*}{2}(1-\cos\theta^*)$ requires a highly virtual

Fig. 9

Hadron-Pomeron subprocess for soft (a) and hard (b) scattering.

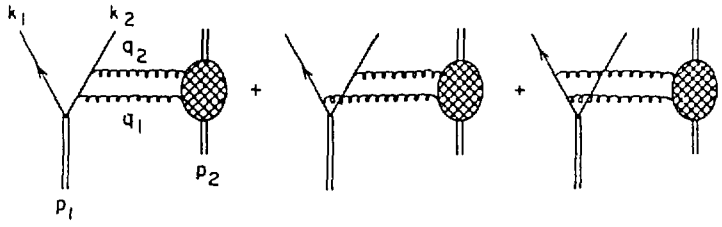

Fig. 10

Two gluon exchange mechanism for (hard) diffractive dissociation.

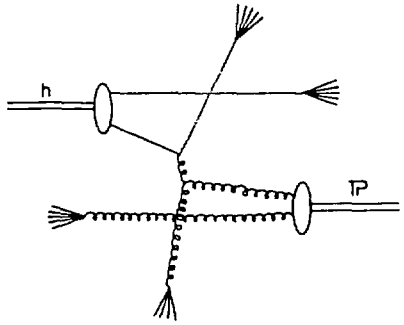

Fig. 11

A hard scattering which leads to more than two jets in the X subsystem.

quark and thereby insures that at least part of the process is short-distance. There are other hard subprocesses of the same order in α_s as $ggM \to q\bar{q}$, hard scattering mechanisms as occur in ordinary h-h collisons, but such mechanisms would not lead to visible high $p_\perp^*$ jet structure at available values of s^*. One such mechanism, leading to two high $p_\perp^*$ parton jets plus the beam and target jets, is shown in fig. 11. Note that the $ggM \to q\bar{q}$ type of mechanism, with two high $p_\perp^*$ jets only (no beam or target jets) is not possible in normal h h collisions-until one constructs a glueball beam (or target).

The cross sections for $hp \to q\bar{q}p$ have been calcualted [40]. Even without a full calculation, scaling laws can be written for the $ggh \to q\bar{q}$ cross section, which in turn lead to [37,41]

$$\frac{d\sigma(hp\to q\bar{q}p)}{dM^2\, d\cos\theta^*} \sim M^{-n_h}, \quad \frac{M^2}{2}(1-\cos\theta^*) \text{ large}, \tag{22}$$

with $n_\gamma = 4$, $n_{\pi,K} = 6$, $n_p = 8$ - where of course for h = p the final state is qq+q+p rather than $\bar{q}$+q+p. Typical results of the full calculation [40] are shown in fig. 12 including an estimate of an overall normalization.

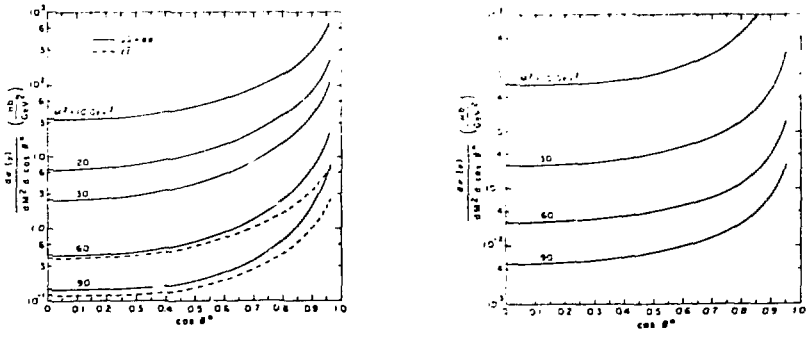

Fig. 12

The estimated cross sections are large enough to measure but the experimental difficulty so far has been to determine the jet axis accurately enough to know that the flattened $\cos\theta^*$ distribution is not just a smearing of the soft jets' exponential distribution.

We therefore have a picture in which we expect soft hadronic jets at small $(1-\cos\theta^*)$, fig. 9a, and hard $q\bar{q}$ (or $qq+q$) jets at large θ^*. How can one distinguish between the soft and hard jets? Gross features such as multiplicity may not be sufficient. All jets tend to look much like $p_\perp$-limited phase space [42]. (For a very nice experimental demonstration of the futility of distinguishing different type jets by their average multiplicity, see [43].) The two ways to tell in $h\bar{P} \to X$ are detailed flavor studies and M^2 dependence at fixed $\cos\theta^*$ (or t^*). The soft cross section has a different M^2 dependence than the hard $q\bar{q}$ cross section, $1/M^2$ for small θ^* vs. eq. (22) for large θ^*. Certain flavor cross sections are an even more obvious indication, if they can be measured. By studying $d\bar{N}/dx_F^*$ in the forward jet as a function of M^2 and/or t^*, one can watch for the vanishing of the forward peak in the $h\bar{P}$ system (e.g. $\pi^+ \to \pi^+X$). As long as it persists one is not looking at $q\bar{q}$ jets. Another possibility (for photoproduction) is to look for differences between quantities measured in one jet and their charge conjugates in the other. Such differences vanish for $\gamma\bar{P} \to q\bar{q}$ but not for $\gamma\bar{P} \to \gamma^*\bar{P}^*$. (Or look for net charge difference between jets, which vanishes for $\gamma^*\bar{P}^*$ but not $q\bar{q}$.)

A very interesting footnote on the soft fragmentation is that the Pomeron fragmentation region should be rich in gluonium states. (For details see [37].)

What does one learn from such diffractive dissociation studies? Assuming the hard jets can be isolated, there are a number of interesting points. Study of the M^2 dependence for the hard jets will test dimensional counting and will reveal the different underlying structures of different beams, γ vs. M vs. B. For incident mesons one has the opportunity to study jets of a known flavor [44], u and $\bar{d}$ from π^+, u and $\bar{s}$ from K^+, etc. And of course by studying Pomeron fragmentation we can hunt for glueballs and also learn something of the valence structure of the Pomeron (e.g. two-gluon vs. three-gluon component).

III. POMERON STRUCTURE

A. Theory

Having accepted the fact that diffractive scattering is intimately connected to gluon exchange (or "derived" the fact by perturbative studies) one would obviously like to sum all possible gluon exchanges. (Even such an ambitious project could miss important nonperturbative effects.) Failing that, one could try to find a "good" subset of graphs - one with such desirable properties as leading s dependence, leading g^2 dependence, unitarity. Having identified such a subset one would attempt to sum it.

Most such studies utilize the Higgs mechanism to give the gluons a mass. This removes the infrared problems of the theory, but it also means the theory is not QCD. One must take the $\mu \to 0$ limit to regain QCD - assuming the limit exists and hoping it is the same as the $\mu = 0$ theory. Considering qq scattering in such a broken theory, it was shown that in the leading log approximation (LLA) the gluon Reggeizes [45,46,47]. The resultant trajectory (which, remember, has gluon quantum numbers) was then inserted into Reggeon Field Theory (RFT) and the part of the amplitude corresponding to vacuum quantum numbers exchanged was extracted. It exhibited the rather disconcerting s-dependence of a fixed cut to the right of $j = 1$, i.e.

$$\sigma_{tot} \sim s^{1-\alpha} \sim s^{\omega_0}, \quad \omega_0 = \frac{2g^2 N}{\pi^2} \ln 2 \qquad (23)$$

violating the Froissart bound. The problem can be traced to the failure of the LLA to maintain unitarity. This can be seen by noting that the elastic amplitude squared contains vacuum exchange,

$$|\mathcal{M}_{el}|^2 = \left| \text{[G]} + \text{[G]} + \cdots \right|^2$$

whereas its discontinuity contains only the Reggeized gluon exchange, and no Pomeron,

$$\text{Disc } \mathcal{M}_{el} \sim \text{[G]} + \text{[G]} + \cdots$$

$$\sim |\text{[G]}|^2 + |\text{[G]}|^2 + \cdots$$

It is therefore necessary to go beyond the LLA. In addition, it is still necessary to take the $\mu^2 \to 0$ and $x \to 0$ limits.

These last two problems are best attacked in color singlet scattering, and recent efforts to go beyond the LLA also have been made in this context. For the $\gamma(q^2) + h$ elastic amplitude, the graphs contributing in the LLA, in the appropriate (axial) gauge, are the ladder graphs,

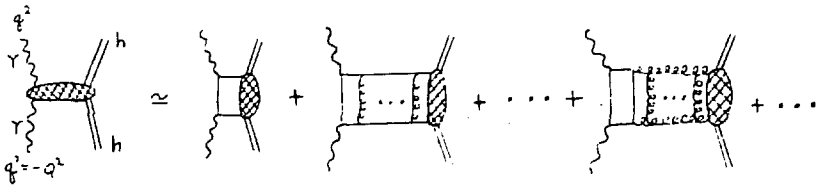

Working in the deep inelastic limit, $x = Q^2/s$ fixed, $s \to \infty$, $\alpha_s \ln x^{-1}$ small, summing these graphs reproduces the standard results for the structure functions [48]. The kinematic region of interest for high energy hadronic diffractive scattering, the Regge limit, is $Q^2 = xs$ fixed (and small) and $s \to \infty$, consequently $x \to 0$. For nonsmall x, the weak coupling results ($g^2 \to 0$, $g^2 \ln s = 1$) inserted into RFT are as in quark-quark scattering, i.e. a

total cross section which grows as s^{ω_0} [47]. If more than two gluons are allowed in the exchange channel, then the range (ln x) of applicability and the s dependence both improve, but x still cannot become too small. The cross section seems to behave as $\sigma(\gamma^*) \sim (\ell n\ x^{-1})^{\eta}_{j}$ $\eta < 2$ [49].

The question of what happens as x, $\mu^2 \to 0$ is exceedingly difficult, and has not yet been fully resolved. The work of A. White represents the most ambitious attempt in this direction [50]. His approach is to start with the "known" perturbative results in the region of their validity (x, $\mu^2 \neq 0$) and to use dispersion relations and unitarity to continue into the $\mu^2 = 0$, small-x regime. Not too surprisingly, in the process of this continuation he finds it necessary to grapple with the problems of confinement and chiral symmetry breaking as well. As the dust settles he sees the following results emerging (for SU(3)). If $\mu \neq 0$ then one obtains a supercritial Pomeron. In the $\mu \to 0$ limit σ_{tot} falls as $s \to \infty$ for the number of flavors less than sixteen. If the number of flavors is equal to sixteen, a critical Pomeron results. Aesthetically this is a particularly attractive result because it has many specific predictions [51]. Asymptotically, it predicts

$$\sigma_{tot} \sim (\ell n\ s)^{-\gamma}, \quad \gamma = -0.26$$

$$\sigma_{el} \sim (\ell n\ s)^{-0.6},$$

$$B \sim (\ell n\ s)^{1.13}$$

$$\frac{d\sigma_{el}}{dt} \sim \frac{d\sigma_{el}}{dt}(t=0) \times F(t(\ell n\ s)^{1.13}). \tag{24}$$

Empirically, the last of these predictions is satisfied quite well, and the prediction for B is consistent with the data, but the s dependence of σ_{tot} and σ_{el} are wrong at present energies (which are not asymptotic of course).

A more conservative approach has been used by Bartels [52], who also presents an intuitive physical picture. He attempts to sum the set of graphs

of the form

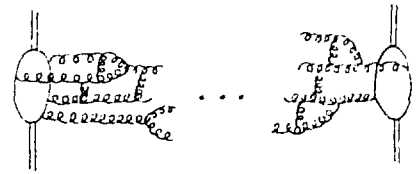

assuming that the set is fully unitary asymptotically. The external particles are color singlets, for which it has been shown [53] that the $\mu \to 0$ limit is finite if the number of gluons in the t channel is conserved. (This illustrates the necessity of treating color singlet scattering.) It is assumed that the limit is also finite even if the number of gluons changes, provided one maintains external color singlets. Bartels then investigates the behavior of the sum of diagrams using a diffusion formalism. Taking $x \to 0$ carries one outside the radius of convergence of the series. In order to define the series in this limit it is necessary to add a nonperturbative term of the form $\exp(-1/g^2)$. The total cross section then has the form

$$\sigma_{tot} \sim \text{const} \times s^{\omega}, \quad \omega \sim 0(e^{-1/g^2}), \tag{25}$$

for small g^2. When g^2 is not small he obtains

$$\sigma_{tot} \sim \text{const} \times [s^{0} + 0(\ell n\ s\ e^{-c/g^2})], \tag{26}$$

but there could be additional as yet undetermined powers of ln s. It is interesting to note that the rise of the total cross section is due to the nonperturbative term, $\exp(-c/g^2) \times \ell n\ s$.

The physical picture of why the cross section rises starts with the old parton model concept that it is the slow (wee) partons which interact in a high energy hadronic collision [54]. If a fast quark is incident it must cascade down to slow quarks and gluons in order to interact, thereby

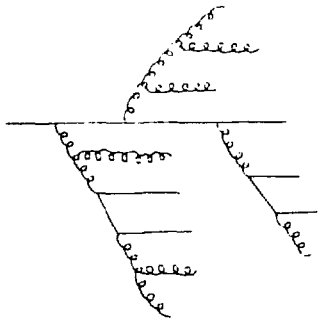

generating its own sea. The transverse spatial extent of this attendant cloud can be estimated as follows. At step i of the cascade some typical perpendicular momentum, $k_{\perp i}$, is transferred, leading to a spatial smearing of order $\Delta b_i = 1/k_{\perp i}$. Since each step in the cascade reduces the rapidity by about one unit, the number of steps required to get slow partons is proportional to the rapidity $N \sim Y$. Viewing the cascade as a random walk in impact parameter space leads to

$$R \sim \Delta b_{tot} \sim \langle \Delta b_i \rangle \times \sqrt{Y} \Rightarrow \sigma_{tot} \sim R^2 \sim \ell n\ s. \qquad (27)$$

A potential problem of such a picture is that in theories with massless particles the Δb_i can be very large and $\langle \Delta b_i \rangle$ can grow with Y, leading to $R \sim \exp(\text{const} \times Y)$. This could be expected to occur in QCD if the gluons appeared in the physical spectrum. The function of the nonperturbative term which was added is to include the effects of confinement and remove massless quanta from the physical spectrum, thereby restoring something like eq. (27). It is still possible that $\langle \Delta b_i \rangle$ could be dependent on N (and hence Y) and could modify the $\ell n\ s$ growth of the cross section. In addition, the fact that the radius was proportional to $\sqrt{Y}$ was due to the random walk having no preferred direction, $\langle \Delta \vec{b}_i \rangle = 0$. If there were some preferred direction (e.g. toward the other incident hadron) then $\langle \Delta \vec{b}_i \rangle \neq 0$ and $R \sim N \sim \ell n\ s$.

We therefore have a qualitative picture of how the hadron radius could grow with energy. This picture is primarily peturbative, with nonperturbative effects preventing the gluons from propagating "too far" as massless particles. These nonperturbative effects appear to control the growth of the

cross section [55] and are most important at larger distance (near the periphery of the hadron?). To construct a full quantitative foundation for *this picture - assuming it is correct - will require a great amount of* additional effort and ingenuity.

B. Phenomenological Notes

Because the preceding discussion of Pomeron structure was quite qualitative, and because other speakers have covered multiparticle production, we shall not spend much time on confrontation of Pomeron models with data, especially multiparticle data. There are, however, a few points which need to be made.

The first is the question of the applicability of asymptotic predicitons of RFT, such as the scaling laws mentioned in connection with the critical Pomeron. If some set of exchanges of fundamental fields yields an elastic amplitude having the form of a Regge pole exchange, e.g.

$$\mathcal{M}_o = i\gamma e^{ct} s^{\alpha_o + \alpha' t} \ , \qquad (28)$$

then RFT provides a formalism for computing the full elastic amplitude resulting from multiple exchanges of this "bare Pomeron" [56,51],

$$\mathcal{M}_{el} = i\gamma s^{\alpha_c} \sum_{n=1}^{\infty} \exp\left[(c+\alpha' \ell n\ s)t/n\right] S_n \ ,$$

$$S_n = \frac{1}{n!} \left[\frac{\gamma\, s^{\alpha_o - 1}}{8\pi (c + \alpha' \ell n\ s)} \right]^{n-1} \ . \qquad (29)$$

The asymptotic behavior of the elastic amplitude depends on the bare intercept α_o. There is some critical value $\alpha_c = 1+\delta$, where δ is small but not known, such that if $\alpha_o > \alpha_c$ (supercritical) the total cross section rises like $\ell n^2 s$. If $\alpha_o < \alpha_c$, the total cross section falls asymptotically. For the critical case, $\alpha_o = \alpha_c$, calculable critical exponents control the asymptotic behavior of not just the total cross section but also a number of other measureable

quantities, such as those given in eq. (24). While some of these predictions agree (or do not disagree) with present experiments, the predictions for the total and elastic cross sections (cf. fig. 1) indicate that either we are not at asymptotic energies or the critical Pomeron is not nature's choice.

Detailed phenomenological studies confirm this [6,57], requiring large nonasymptotic corrections or agreeing with a perturbative expansion. The point of the perturbative expansion is that at "low" energies only the first few terms in eq. (29) are important. (Also, effects of flavor thresholds have a significant impact on the effective α_o appropriate at a given s.) Another indication that at present (through collider) energies exchange of only a few bare Pomerons is relevant rather than the full sum of (29) comes from analysis of multiplicity distributions [58]. Again it is found that only the first few terms in (29) are important. Therefore, indications are that we are not in (or close to) the asymptotic regime of RFT scaling laws.

In connection with multiparticle production, it is not hard to see how one can make contact with phenomenologically successful models, such as those reviewed by other speakers at this conference [1]. Considering 2GE as an example, the discontinuity in the elastic amplitude leads to

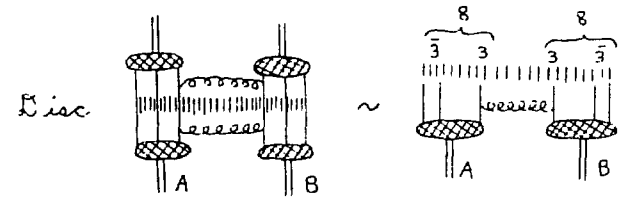

where the series of short vertical lines represents confining effects. The two separating subsystems are joined by color fields and can hadronize according to one's favorite model, e.g. the 3 and $\bar{3}$ from different hadrons can pair off, forming two chains or strings and producing the multiparticle final state of the dual parton model (for one bare Pomeron exchange).

IV. SURMISE AND SUMMARY

Recalling the features of diffractive scattering which were presented in the Introduction as requiring explanation, we can draw up the summary of Table III. A check mark indicates that the feature is understood or explained in the context of a QCD-based model such as 2GE or ladder exchange. A check with a slash through it indicates that the feature is understood within some model whose connection with QCD is more obscure.

At a fixed energy the shapes of elastic differential cross sections are well described by optical models. The energy dependence of virtually all relevant quantities - σ_{tot}, B, σ_{el}, t_{dip}, $\eta(b=0)$ - is consistent with the hypothesis of geometrical scaling (GS), although that does not address the question of the energy dependence of the scale $R(s) \equiv [\text{const} \times \sigma_{tot}(s)]^{1/2}$. In addition, the relative magnitudes of total cross sections are reproduced by geometrical considerations or by 2GE. The problem is to obtain a geometrical model from QCD - or at least to see how such a model might follow from QCD.

The more ambitious goal of deriving an optical model from QCD is beyond our present grasp, of course. However, I think we have some insight into how it can occur. If we consider 2GE between color singlet bound states as a paradigm for how confined bound states scatter perturbatively, then we immediately obtain the correct results for the relative sizes of total cross sections, and they have a geometrical interpretation. In addition, 2GE yields helicity conservation, approximate factorization, small Re f_{el}/Im f_{el} ratio, and constant s dependence for the total cross section. Even if we can treat the scattering as incident wave functions plus perturbative mechanism we must go beyond 2GE for the perturbative mechanism, including at least leading logs; but it is easy to see that most of the successes just mention will carry over

Table III

Feature	Understood?	How
1) $\sigma_{tot} \sim$ const	✓	2GE, ...
$\sim (\ln s)^2$	✗	---
2) $\sigma_{el} \sim \epsilon\sigma_{tot}$	✓✗	GS, Low picture
3) Re/Im small	✓	2GE, ...
4) forward peak	✓✗	optical models+GS
5) factorization	✓	2GE, ...
6) additivity	✓	2GE...
7) multiparticle cross sections	✓✗	dual parton, ...
8) Etc.: helicity nonflip	✓	2GE, ...
diffractive excitation	not yet	---
dip	✓✗	optical models+GS
slope break	✓✗	optical model
inclusive	✓	miscellaneous
		parton models

to more complicated graphs if the final coupling to the external hadrons is through two gluons. We also must still show that we obtain the characteristic diffraction pattern for the differential cross section.

Regarding the question of whether the problem can be treated by lumping nonperturbative effects into initial and final wave functions and then treating the scattering of the quarks perturbatively, it is quite clear that that can not be entirely correct. There are also nonperturbative effects in the exchange channel: confinement prevents gluons from propagating through space as massless particles. These effects determine the spatial extent of the cloud of soft partons surrounding incident valence quarks, they determine (are determined by) the size of hadrons at a given s. We therefore expect the effective size of the hadron (and therefore the growth of σ_{tot}) as a function of s to be fixed nonperturbatively. For peripheral collisions then, the situation will be very complicated, but in the interior of the hadron (smaller b) the wave functions plus perturbative scattering may be sufficient.

Of course it is possible that the scenario just outlined is hopelessly optimistic and that a viable description of diffractive scattering will require a full-blown nonperturbative approach. However, the results obtained from a simple model so far are sufficiently encouraging, and the prospect of a "proper nonperturbative" solution sufficiently remote, that it seems worthwhile to try to advance with a hybrid model such as the one above. In that case the two most pressing questions are whether an optical model type of differential cross section does result and why does the total cross section grow like $\ln^2 s$.

ACKNOWLEDGMENTS

During the course of preparing this talk and paper I have benefitted considerably from conversations with B. Anderson, P. Aurenche, J. Cumalat, and T. DeGrand. I am also grateful to the organizers of this meeting for a pleasant and useful week. This work was supported by the U.S. Department of Energy, Grant No. DE-AC02-81ER40025.

REFERENCES

1. B. Anderson, these proceedings;
A. Capella, these proceedings.
2. D. Lloyd Owen, in "Particles and Fields - 1982 (APS/DPF University of Maryland)," eds. W. Caswell and C. Snow (AIP, New York, 1983).
3. A. S. Carroll et al., Phys. Lett. 61B, 303 (1976); Phys. Lett 80B, 423 (1979); UA4 Collab., R. Battiston, Phys. Lett. 117B, 126 (1982).
4. M. Ambrosio et al., Phys. Lett. 115B, 495 (1982).
5. J. Velasco, these proceedings.
6. J. W. Dash, S. T. Jones, and E. Manesis, Phys. Rev. D18, 303 (1978); J. W. Dash and S. T. Jones, Marseille preprint CPT 82/1451 (1982).
7. D. S. Ayres et al., Phys. Rev. D15, 3105 (1977).
8. J. P. Burq et al., CERN-EP/82-15 (1982); U. Amaldi et al., Phys. Lett. 66B, 390 (1977).
9. N. Amos et al., Phys. Lett 120B, 460 (1983).
10. UA4 Collab., R. Battiston et al., Phys. Lett. 115B, 333 (1982).
11. M. M. Block and R. N. Cahn, Phys. Lett. 120B, 229 (1983).
12. C. Conta et al., Nucl. Phys. B175, 97 (1980).
13. pp, $\bar{p}p$, πp, Kp: A. S. Carroll et al., Phys. Rev. Lett. 33, 928 (1974), Phys. Rev. Lett. 33, 933 (1974);
Σp, Ξp: S. F. Biagi et al., Nucl. Phys. B186, 1 (1981);
ϕp: R. M. Egloff et al., Phys. Rev. Lett. 43, 657 (1979);
R. M. Egloff, University of Toronto thesis (1978).
14. E. M. Levin and L. L. Frankfurt, Sov. Phys. JETP Lett. 2, 65 (1965);
H. J. Lipkin and F. Scheck, Phys. Rev. Lett. 16, 71 (1966);
J. J. J. Kokkedee and L. Van Hove, Nuovo Cim. 42, 711 (1966).

15. P. Carlsson, these proceedings;
UA5 Collab., K. Alpgård et al., Phys. Lett. 121B, 209 (1983);
UA1 Collab., G. Arnison et al., Phys. Lett. 123B, 108 (1983).

16. Z. Koba, H. B. Nielsen, and P. Olesen, Nucl. Phys. B140, 317 (1972);
P. Slattery, Phys. Rev. D7, 2073 (1973);
E. H. DeGroot, Phys. Lett. 57B, 159 (1975);
W. Thomé et al., Nucl. Phys. B129, 365 (1977).

17. F. C. Winkelmann et al., Phys. Rev. Lett. 32, 121 (1974);
J. Armitage et al., Nucl. Phys. B194, 365 (1982).

18. G. Gustafson, in "Proceedings of the IX International Winter Meeting on Fundamental Physics," ed. A. Ferrando (Instituto de Estudios Nucleares, Madrid, 1981).

19. U. Amaldi et al., Phys. Lett. 44B, 112 (1973).

20. U. Amaldi and K. R. Schubert, Nucl. Phys. B166, 301 (1980).

21. J. Dias de Deus, Nucl. Phys. B59, 231 (1973);
A. Buras and J. Dias de Deus, Nucl. Phys. B71, 481 (1974).

22. T. T. Chou and C. N. Yang, Phys. Rev. 170, 1591 (1968); Phys. Rev. D19, 3268 (1979).

23. F. E. Low, Phys. Rev. D12, 163 (1975);
S. Nussinov, Phys. Rev. Lett. 34, 1286 (1975), Phys. Rev. D14, 246 (1976).

24. J. F. Gunion and D. E. Soper, Phys. Rev. D15, 2617 (1977).

25. H. J. Lipkin, Phys. Lett. 116B, 175 (1982).

26. P. Ensign and J. Randa, in preparation.

27. R. H. Dalitz, in "Fundamentals of Quark Models," Proceedings of the Seventeenth Scottish Universities Summer School, eds. I. M. Barbour and A. T. Davies (SUSSP, Edinburgh, 1977).

28. N. Isgur, in "The New Aspects of Subnuclear Physics," ed. A. Zichichi (Plenum, NY and London, 1980); and in "New Flavours and Hadron Spectroscopy," ed. J. Tran Thanh Van (Editions Frontieres, Dreux, France, 1981).

29. N. Isgur and G. Karl, Phys. Lett. 72B, 109 (1977); Phys. Lett. 74B, 353 (1978); Phys. Rev. D19, 2653 (1979); Phys. Rev. D20, 1191 (1979).

30. C. Quigg and J. L. Rosner, Phys. Rep. 56, 167 (1979).

31. H. I. Miettinen and J. Pumplin, Phys. Rev. Lett. 42, 204 (1979);
A. Bialas and E. Bialas, Phys. Rev. D21, 675 (1980);
EMC Collab., H. E. Montgomery, in "Particles and Fields - 1982 (APS/DPF University of Maryland)," eds. W. Caswell and G. Snow (AIP, NY, 1983).

32. M. Binkley et al., Phys. Rev. Lett. 50, 302 (1983);
M. S. Atiya et al., Phys. Rev. Lett. 43, 1691 (1979);
D. Aston et al., Phys. Lett. 92B, 215 (1980);
A. Clegg, in "New Flavours and Hadron Spectroscopy," ed. J. Tran Thanh Van (Editions Frontieres, Dreux, France, 1981).

33. E. M. Levin and M. G. Ryskin, Yad. Fiz. 34, 1114 (1981) [Sov. J. Nucl. Phys. 34, 619 (1981)].

34. A. Chodos et al., Phys. Rev. D9, 3471 (1974); D10, 2599 (1974);
T. DeGrand et al., Phys. Rev. D12, 2060 (1975);
K. Johnson, Acta Phys. Polonica B6, 865 (1975).

35. K. Gulamov, N. Sadykov, and A. Tarasov, Report #E2-82-501, JINR, Dubna (1982).

36. J. Pumplin and E. Lehman, Z. Phys. C9, 25 (1981).

37. T. DeGrand and J. Randa, Phys. Lett. 110B, 484 (1982).

38. B. R. Desai and U. Sukhatme, Riverside preprint UCR-82-3 (1982).

39. M. G. Albrow et al., Nucl. Phys. B108, 1 (1976);
D. S. Ayres et al., Phys. Rev. Lett. 37, 1724 (1976);
R. L. Anderson et al., Phys. Rev. Lett. 38, 880 (1977);
Y. Akimov et al., Phys. Rev. Lett. 39, 1432 (1977).

40. S. F. King, A. Donnachie, and J. Randa, Nucl. Phys. B167, 98 (1980);
J. Randa, Phys. Rev. D22, 1583 (1980).

41. G. Bertsch et al., Phys. Rev. Lett. 47, 297 (1981).

42. A. Clegg and A. Donnachie, Z. Phys. C13, 71 (1982).

43. B. Pietrzyk et al., Phys. Lett. 113B, 105 (1982).

44. S. P. Misra, A. R. Panda, and B. K. Parida, Phys. Rev. Lett. 45, 322 (1980).

45. L. Tyburski, Phys. Lett. 59B, 49 (1975); Phys. Rev. D13, 1107 (1976);
B. M. McCoy and T. T. Wu, Phys. Rev. D12, 3257 (1976);
L. N. Lipatov, Sov. J. Nucl. Phys. 23, 642 (1976);
H. Cheng and C. Y Lo, Phys. Rev. D13, 1131 (1976); Phys. Rev. D15, 2959 (1977).

46. J. B. Bronzan and R. L. Sugar, Phys. Rev. D17, 585 (1978).

47. E. A. Kuraev, L. N. Lipatov, and V. S. Fadin, Sov. Phys. JETP 45, 199 (1979).

48. C. H. Llewellyn Smith, Phys. Lett. 79B, 83 (1978).

49. L. V. Gribov, E. M. Levin, and M. G. Ryskin, Phys. Lett. 110B, 185 (1981).

50. See, e.g., A. R. White, in "Multiparticle Dynamics 1982," eds. W. Kittel, W. Metzger, and A. Stergiou (World Scientific, Singapore, 1982).

51. H. Abarbanel, J. Bronzan, R. Sugar, and A. White, Phys. Rep. 21, 119 (1975);
M. Moshe, Phys. Rep. 37, 255 (1978).

52. J. Bartels, Acta. Phys. Polon. B11, 281 (1980); DESY 80/54 (1980).

53. J. Bartels, Nucl. Phys. B175, 365 (1980).

54. R. Feynman, "Photon-Hadron Interactions" (W. A. Benjamin, Reading, MA, 1972).

55. For a differing view, see R. Peschanski, these proceedings; or G. Cohen-Tannoudji, H. Navelet, and R. Peschanski, Phys. Rev. D, to be published (1983).

56. V. N. Gribov, Sov. Phys. JETP 26, 414 (1968).

57. J. Baumel, M. Feingold, and M. Moshe, Nucl. Phys. B198, 13 (1982);
J. Dash, Marseille preprint CPT-82/1405 (1982).

58. P. Aurenche and F. Bopp, Phys. Lett. 114B, 363 (1982);
A. Capella and J. Tran Thanh Van, Phys. Lett. 114B, 450 (1982);
A. Kaidalov, Phys. Lett. 116B, 459 (1982).

DISCLAIMER